

AN IMPROVED PROCEDURE FOR ENERGY MATCHING BETWEEN PS AND SPS AT CERN

G. Papotti*, S. Cettour Cavé, F. Follin, A. Spierer, CERN, Geneva, Switzerland

Abstract

Energy matching between two hadron synchrotrons is the adjustment of the magnetic bending fields and beam momentum to obtain a correct transfer between the two. Conventionally, energy matching is achieved by turning off the RF system and measuring the revolution frequency of the de-bunching beam in the receiving accelerator. For an ideal circumference ratio, the orbits would then be centred in the two rings. However, this procedure is non-transparent, seen that the de-bunched beam cannot be accelerated anymore. Thanks to the Low-Level RF (LLRF) upgrade in the Super Proton Synchrotron (SPS) during the 2019-2021 long shutdown, most LLRF signals have become available in digital form, allowing easy online display, analysis, and storage. In this contribution, we look at the possibility of performing energy matching between the PS and the SPS in a more transparent way, without disabling the RF system. The signals from the beam phase and synchronization loops reveal information on the energy of the beam injected into the SPS. This allows to continuously monitor the transfer frequency error, as well as identify and correct potential long-term drifts.

INTRODUCTION

The particle momentum p at transfer between two hadron synchrotrons is the same for the two machines, and this imposes conditions on the choice of the magnetic field B and orbit in the two accelerators to simultaneously satisfy Eq. 1 [1]:

$$\frac{p}{e} = \rho_0 \left(\frac{R}{R_0} \right)^{\frac{1}{\alpha_p}} B \quad (1)$$

where e is the particle charge, ρ_0 is the bending radius, R is the mean orbit radius and R_0 is the same quantity for the perfectly centered orbit (i.e. the nominal orbit), and α_p is the momentum compaction factor ($\alpha_p := p/R (\partial R/\partial B)_B$). Energy matching between two hadron synchrotrons is the optimisation of such transfer, by adjusting p and B in the two accelerators, ideally to keep the beam onto the nominal orbit ($R = R_0$).

A transfer at fixed frequency has the advantage of providing a reproducible reference point. With the transfer frequency fixed, and imposing the constraint to inject onto the central orbit, results in p to be chosen, thus also B in the two accelerators, via Eq. 1.

In general, though, a transfer frequency offset Δf and a mean radial position offset ΔR can be measured. Energy matching is generally an optimisation around the working

point: Eq. 1 is derived with respect to p , R , and B to infer the well known set of differential equations that relate small deviations in the three quantities [1].

A well defined procedure for energy matching at fixed frequency has been long in place for the CERN smaller synchrotrons [2]. This procedure is based on Eqs. 2 and 3, here applied to the Proton Synchrotron (PS, sending machine), and the Super Proton Synchrotron (SPS, receiving machine).

$$\Delta B_{\text{PS}} = -B_{\text{PS}} \left(\gamma^2 - \gamma_{\text{tr,PS}}^2 \right) \left(\frac{\Delta f_{\text{SPS}}}{f} + \frac{\Delta R_{\text{SPS}}}{R_{\text{SPS}}} \right) \quad (2)$$

$$\Delta B_{\text{SPS}} = -B_{\text{SPS}} \left(\frac{\gamma^2 \Delta f_{\text{SPS}}}{f} + \left(\gamma^2 - \gamma_{\text{tr,SPS}}^2 \right) \frac{\Delta R_{\text{SPS}}}{R_{\text{SPS}}} \right) \quad (3)$$

In Eqs. 2 and 3, ΔB is the proposed correction to the bending field B , γ is the Lorentz factor, γ_{tr} is gamma transition, and f is the transfer frequency (most quantities are defined per accelerator, PS or SPS). The conventional procedure, described in [2], is performed by measuring, at the receiving machine, the mean radial offset ΔR_{SPS} by means of the beam position monitors, and the transfer frequency error Δf_{SPS} . In particular, Δf_{SPS} is measured by looking at the beam drift with respect to the set transfer frequency by turning the RF off. This makes the procedure non-transparent to operation, as the beam cannot be accelerated and thus not used for physics production.

In this paper we derive the frequency error from the Synchronization Loop (SL) error in Low Level RF system [3]. This can be done transparently to beam operation, i.e. without turning the RF off. In addition, thanks to the digital LLRF implementation, the SL error can be easily acquired in higher level controls, together with the radial offset position from the global orbit measurement. An implementation that allows for continuous monitoring of the error in energy matching between the PS and SPS is in place since the end of the 2022 run. We also report preliminary and interesting observations, e.g. the dependence of the proposed corrections for energy matching on the supercycle composition.

FREQUENCY ERROR MEASUREMENT

In the LLRF beam control, the SL [4] controls the average revolution and hence RF frequencies so that they follow the reference frequency (derived from the bending field or from a programmed function). At SPS injection, where energy matching is performed, the SL is locked on the transfer frequency, for correct synchronization to the previous machine, in the case of “bunch-to-bucket” transfer [4].

The SL is by design much slower (i.e. has a much smaller gain) than the beam phase loop, which locks the phase of

* giulia.papotti@cern.ch

the accelerating wave to the circulating bunches. The small gain guarantees the adiabaticity of the frequency change. This means also that, early after injection, the frequency correction by the loop will still be small, and that the SL error signal can then be taken as a measurement of the difference between the reference frequency and the incoming beam energy, or frequency, i.e. the desired quantity Δf_{SPS} in Eqs. 2 and 3.

However, one cannot take the very first turns into account, during which the SL error is dominated by the phase loop response to the injection transients. In the practical implementation, the phase error difference $\Delta\phi$ was acquired from the SL error over a time span of $\Delta T_{\text{turns}} = 10$ turns (e.g. between turns 15 and 25 after injection), and the Δf_{SPS} calculated according to Eq. 4:

$$\Delta f_{\text{SPS}} = \frac{\Delta\phi}{360 \Delta T_{\text{turns}}} f_{\text{rev,SPS}}. \quad (4)$$

An example of the SL error together with the derived frequency error is shown in Fig. 1. The maximum detected frequency error is 220 Hz, while the one detected in our proposed algorithm is 207 Hz.

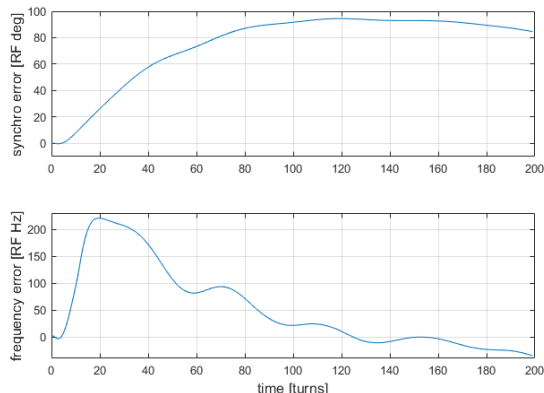


Figure 1: Turn-by-turn SL error (top); frequency error derived according to Eq. 4 (bottom).

As the SL must be closed from injection, the error as calculated above is by definition slightly underestimated. Nevertheless, this algorithm allows for continued monitoring, transparently to operation, so that subsequent corrections could be done. Note that detection a few turns earlier was possible for single bunch beams, but the proposed implementation with later detection is more generic, as it is successful also for multi-bunch beams, for which beam loading correction transients are non-negligible during the first turns.

CONTROLS IMPLEMENTATION

The SPS operation team developed a Java server-GUI pair, the “SPS Quality Check” (SPS QC, [5]) in collaboration with the controls and machine protection groups at CERN. The SPS QC allows monitoring and storage of a number of

parameters pertinent to beam quality, e.g. extracted intensity, transmission, and spill quality on a cycle-to-cycle basis.

Equations 2 and 3 were implemented in a new SPS QC module dedicated to energy matching. The quantities B_{PS} , B_{SPS} , γ , γ_{tr} , and f_{SPS} are retrieved on a cycle-by-cycle basis from the PS and SPS settings database. The Δf_{SPS} is derived from the SL error acquisition according to Eq. 4. The ΔR is calculated by averaging the data published by the Beam Position Monitors (BPMs) in the ring. Possible BPMs with unrealistic readings are not yet excluded by the algorithm, resting on the assumption that their number is proportionally small.

The SPS QC can export relevant parameters to the NX-CALS logging database [6], for long term storage. This allows the follow up of performance achievements, long term drifts, and possible issues throughout the entire accelerator run.

EXPERIMENTAL OBSERVATIONS

The PS and SPS accelerators are driven by a single central timing system, which allows the execution of different beams (“cycles”) either for physics production or destined to a downstream machine, respectively the SPS or the Large Hadron Collider (LHC). Every cycle has a characteristic set of accelerator parameters, and the hardware follows the settings for each cycle as required. A supercycle is a combination of such individual cycles, which are executed sequentially in a pre-programmed order, and repeats periodically. Figure 2 shows an example of SPS supercycle.

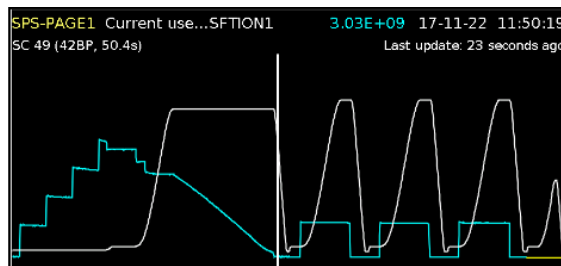


Figure 2: Example of SPS supercycle. In white, the dipole current, proportional to the beam energy; in light blue the beam intensity. A cycle for fixed target ion experiments (with 4 injections and a slow extraction), is followed by three instances of a cycle with a single bunch to be extracted to the AWAKE experiment, and by one short cycle without beam (for magnetic reproducibility).

While the set values for each cycle are identical, in practice some small differences can arise, the most notable example being the magnetic hysteresis of the SPS main dipoles and quadrupoles (and thus the resulting magnetic fields).

For the supercycle in Fig. 2, the effect of the magnetic hysteresis on the energy matching of the AWAKE beam can be seen in Fig. 3: the proposed corrections for ΔB_{SPS} display a 3-fold symmetry, depending on the cycle placement in the supercycle. This corresponds to a scatter in $\Delta p/p$ smaller than 0.05%.

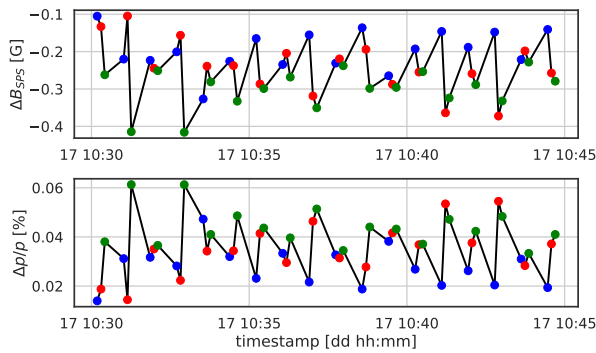


Figure 3: Proposed corrections ΔB_{SPS} for the supercycle shown in Fig. 2 (top), and momentum scatter $\Delta p/p$ of the incoming beam (bottom). The three-fold symmetry is highlighted by the color scheme.

The PS supercycle composition also matters: while the fixed target proton beam is produced with the same PS and SPS cycles, the preceding cycle in the PS has also an impact. Figure 4 displays the proposed corrections for the SPS and PS fields before and after a PS supercycle change at 02:35 on 14 November. The different color code highlights the difference between the first half and the second half of the plots: while in the first part the preceding PS cycles differ (green and blue dots highlight two “families” in the proposed corrections), in the second half the production scheme is fully symmetrical, and the proposed corrections stagger together (the momentum scatter is halved).

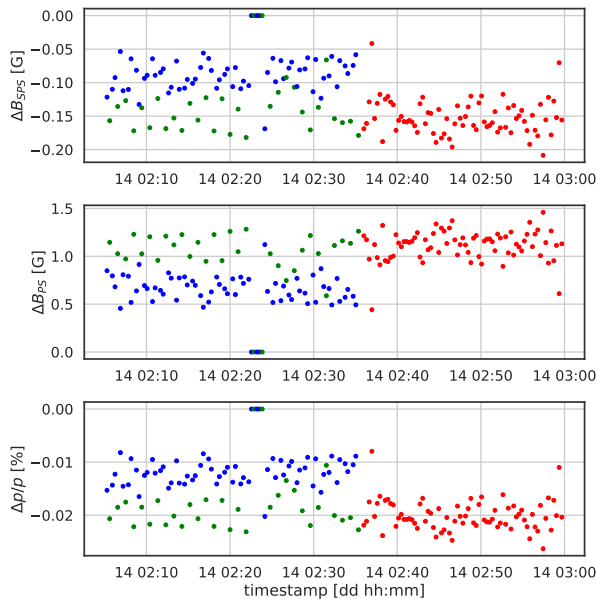


Figure 4: Proposed corrections ΔB_{SPS} (top), and ΔB_{PS} (middle). A supercycle change at the PS at 02:35 on 14 November reduces the two families of proposed corrections ΔB_{SPS} (blue and green) to a single one (red). The resulting momentum spread $\Delta p/p$ is reduced (bottom).

Small effects at circuit restart are also visible, and some tens of minutes are required for the start-up transients to settle (Fig. 5). The main SPS circuits had been off on 12 November in order to allow for an access into the SPS ring, and beam was reestablished at about 17:10. Figure 5 shows the measured Δf_{SPS} (top), ΔR_{SPS} (middle) and the resulting $\Delta p/p$ (bottom): while the scatter on the measurements is non-negligible, the three curves show a slope for the first 15 minutes, before the transients settle.

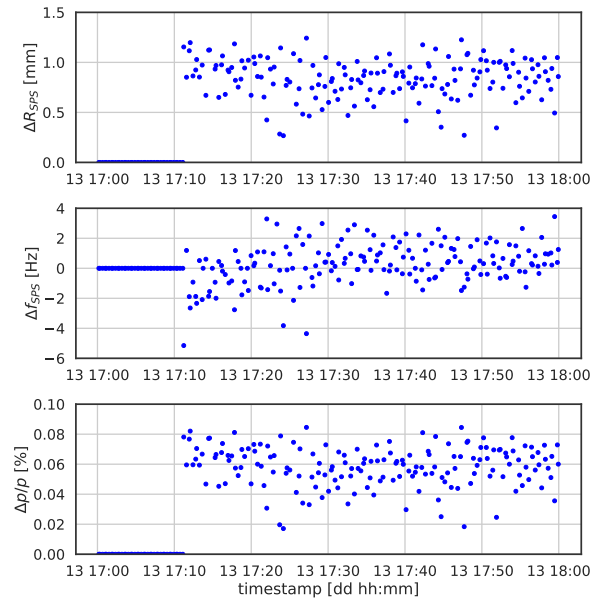


Figure 5: Measured radial error ΔR_{SPS} (top) and frequency error Δf_{SPS} (middle), and resulting momentum scatter $\Delta p/p$ (bottom). Drift visible in the interval 17:10-17:25, transients have settled in the interval 17:25-18:00 on 13 November.

CONCLUSIONS

This paper presents the first automated measurements with proposals for corrections for the PS-SPS energy matching based on transfer at fixed frequency. The algorithms are based on well known physics laws, where a measurement of the incoming beam frequency error and average radial position at the first turn, allow to calculate corrections for the bending fields of the upstream and downstream machine. While the conventional method was based on dedicated measurements with RF off in the downstream accelerator, we use the LLRF synchronization loop error to derive the frequency error, thus making the measurement transparent to operation. The integration in the SPS software tool chain was achieved in the end of the 2022 operation, and revealed first interesting results: the dependence of the proposed corrections on the PS and SPS supercycles, and the evidence of start-up drifts of the SPS main bending field.

REFERENCES

- [1] C. Bovet, R. Gouiran, I. Gumowski, K. H. Reich, “A selection of formulae and data useful for the design of A. G. Syn-

chrotrons”, CERN, Geneva, Switzerland, Rep. CERN/MPS-SI/Int. DL/70/4, 1970.

- [2] M. Benedikt, H. Damerau, S. Hancock, “A Straightforward Procedure to Achieve Energy Matching between PSB and PS”, CERN, Geneva, Switzerland, Rep. CERN AB-Note-2008-042 MD, 2008.
- [3] A. Spierer *et al*, “The CERN SPS Low Level RF: The Beam-Control”, in *Proc. IPAC 2022*, Bangkok, Thailand, Jun. 2023,
- paper TUPOST021, pp. 895-898.
- [4] R. Garoby, “Timing Aspects of Bunch Transfer Between Circular Machines, State of the Art in the PS Complex”, CERN, Geneva, Switzerland, Rep. CERN/PS/RF/Note 84-6, 1984.
- [5] F. Follin *et al*, private communication, Nov. 2022.
- [6] <https://nxcals-docs.web.cern.ch>